

Design of electromagnetic spatial filters exploiting the normal polarization of all-dielectric metasurfaces

Alessio Monti^{*(1)}, Andrea Alù⁽²⁾, Alessandro Toscano⁽¹⁾, and Filiberto Bilotti⁽¹⁾

(1) Department of Industrial, Electronic and Mechanical Engineering, Roma Tre University, 00146 Rome, Italy

(2) CUNY Advanced Science Research Center, New York, USA

Abstract

In this contribution, we discuss the design of spatial filters realized through all-dielectric metasurfaces. Specifically, it is first discussed how the tangential polarizations of all-dielectric metasurfaces can be exploited to design wideband dielectric mirrors. Then, it is shown how it is possible engineering the normal polarization of these structures and use them to open a transmission window around a desired impinging angle. Several examples and realistic full-wave simulations are included to verify the analytical models and the physical discussions.

1. Introduction

Electromagnetic (EM) metasurfaces represent a flourishing research field that is having a strong impact in different technical and scientific communities. Indeed, metasurfaces enable unconventional wave phenomena and allow the design of unprecedented devices [1]. Among the others, all-dielectric metasurfaces based on Mie resonators have been the subject of extensive research efforts because they exhibit a wide gamma of possible scattering response and are generally less lossy than their metallic counterpart [2]-[4].

Despite the interest aroused, most of the current studies about metasurfaces are focused on their analysis and design for normally-incident fields. Conversely, the electrodynamics of metasurfaces for oblique incidence is weakly explored, even though it seems particularly rich and promising for new applications [5]-[7].

In this contribution, we investigate the response of an all-dielectric metasurface for oblique incidence and show how the complex multipolar response of its meta-atoms can be engineered to design an ultra-selective angular filter working even for extreme angles. This effect is obtained by properly combining the resonances of the tangential dipoles and the one due to the normal polarization, occurring only when off-normal incidence is considered.

2. Modelling

The structure we consider in this paper is shown in Fig. 1 and it consists of a regular array of dielectric spheres made by a high-index material with permittivity ϵ_r . We denote with a the radius of each sphere and with d the lattice

constant. We assume the structure is excited by a TE plane wave forming an angle θ_0 with the normal to the metasurface.

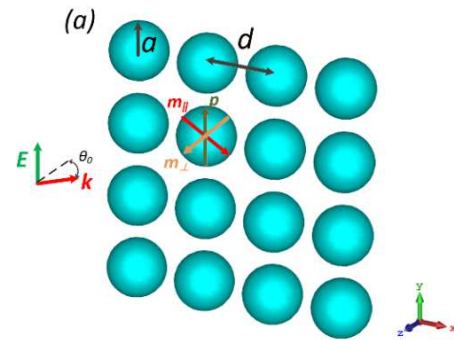


Figure 1. Geometry of the all-dielectric metasurfaces considered in this work. The individual spheres are made by a high-index material and, for oblique incidence, support both tangential and normal polarization currents. The impinging field is a TE(z) plane wave forming an angle θ_0 with the z-axis.

For $\theta_0 = 0^\circ$, the macroscopic behavior of this structure can be fully characterized using a couple of homogenized parameters [8], *i.e.*, the electric surface impedance due to the tangential electric dipole p and the magnetic surface admittance due to the tangential magnetic dipole m_{\parallel} . According with the coupled-dipole approach, these quantities can be written in closed-form as

$$\begin{aligned} \frac{Z_e}{\eta_0} &= -\frac{d^2}{k_0} \left[\text{Im}[\alpha_e^{-1}] - \frac{k_0^3}{6\pi} + i(\text{Re}[\alpha_e^{-1} - \beta_e]) \right], \\ \eta_0 Y_m^{\parallel} &= -\frac{d^2}{k_0} \left[\text{Im}[\alpha_m^{-1}] - \frac{k_0^3}{6\pi} + i(\text{Re}[\alpha_m^{-1} - \beta_m]) \right], \end{aligned} \quad (1)$$

where α_e and α_m are the dynamic tangential polarizabilities of the particles (that can be expressed in terms of the respective Mie scattering coefficients [8]), β_e and β_m are the interaction constant among them (for which several approximated expressions are available [9]) and k_0 and η_0 are the free-space wavenumber and impedance, respectively.

When the structure is excited by an off-normal plane wave, instead, we need also to account for the excitation of

normal dipoles within each meta-atom. As discussed in [10], the effects of a normal polarization can be described by equivalent tangential currents in the homogenization limit. In particular, it is easy to verify that a normal magnetic (electric) dipole radiates symmetrically (anti-symmetrically), similarly to a tangential electric (magnetic) dipole. Therefore, the macroscopic behavior of the metasurface for oblique incidence can be retrieved by defining a symmetric and anti-symmetric surface impedance, which account for the appropriate tangential and normal dipoles excited in each meta-atom. As an example, when the impinging wave is transverse electric (TE), the symmetric surface impedance is the sum of the surface impedance due to the tangential electric dipole and the one due to the normal magnetic dipole, *i.e.*, $Z_{symm} = Z_e + Z_m^\perp$, whereas the asymmetric surface impedance coincides with the sole surface impedance due to the tangential magnetic dipole, *i.e.*, $Z_{asymm} = Z_m^\parallel$.

Once these quantities have been calculated using the coupled-dipole approach discussed above, the reflection and transmission coefficient of the metasurface for an arbitrary impinging angle are given by:

$$\Gamma(\vartheta_0) = \frac{-\eta_0}{2Z_{symm} \cos(\vartheta_0) + \eta_0} + \frac{Z_{asymm}}{Z_{asymm} + 2\eta_0 \sec(\vartheta_0)}, \quad (2)$$

$$T(\vartheta_0) = 1 - \frac{\eta_0}{2Z_{symm} \cos(\vartheta_0) + \eta_0} - \frac{Z_{asymm}}{Z_{asymm} + 2\eta_0 \sec(\vartheta_0)}.$$

3. Design of angular filters

In Fig. 2 and Fig. 3, we report the symmetric and anti-symmetric surface reactance for different angles of incidence of an all-dielectric metasurfaces with parameters: $a = 0.5\lambda$ and $d = 1.28\lambda$, being λ the wavelength inside the high-index dielectric. As it can be appreciated, when normal incidence is considered, the structure exhibits two different resonance peaks (related with the excitation of magnetic and electric tangential dipoles), whose spectral position and quality factors can be engineered to achieve a wide reflection bandwidth [8].

Conversely, for oblique incidences, an additional resonance of the symmetric surface impedance appears. This resonance – which is due to normal magnetic dipole - is placed in-between the tangential resonances and can be exploited to achieve a balanced condition between symmetric and anti-symmetric scatterers and open a transmission window within the mirror bandwidth. The desired angle and operation frequency of the transmission window can be finely tuned by acting on either the geometry or the material permittivity. As an example, once fixed the geometry and the desired transmission angle, it is possible optimizing the permittivity of the high-index material to shift the resonance of the normal polarization at the desired frequency.

To better explain these points, in Fig. 3 we report the reflection and transmission coefficient of the considered high-index metasurface for different values of the permittivity ϵ_r for an excitation angle $\theta_0=80^\circ$. These results have been obtained through realistic full-wave-

simulations. The electromagnetic parameters, which also include realistic losses, have been chosen by considering realistic ceramic materials available at microwaves [11] and even at THz frequencies [12]. At it can be appreciated, the normal polarization sustained by the metasurface allows opening a narrow transmission window within the reflection bandwidth of the mirror. Given their nature, these transmission bands are strongly angular-selective and, as such, can be exploited for spatial filtering purposes.

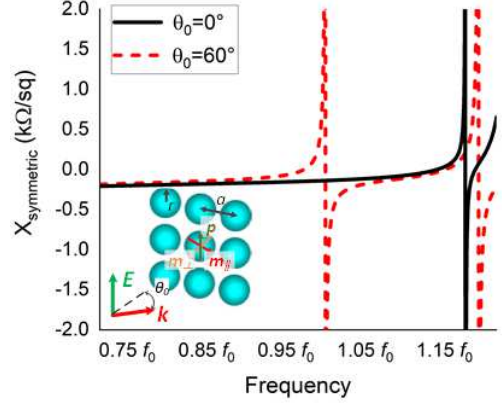


Figure 2. Symmetric surface impedance of an all-dielectric metasurface for different angles of incidence.

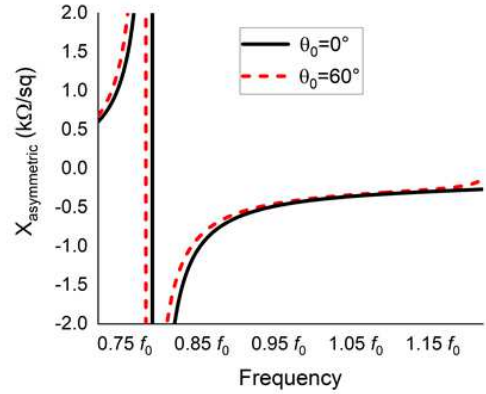


Figure 3. Anti-symmetric surface impedance of an all-dielectric metasurface for different angles of incidence.

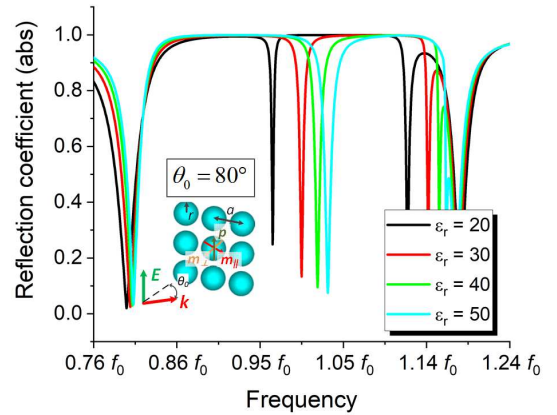


Figure 4. Reflection coefficient of an all-dielectric metasurface excited by a TE plane wave with $\theta_0=80^\circ$ for different values of the material permittivity. A loss tangent equal to 0.001 has been considered in the simulations.

To appreciate the angular selectivity of these devices, in Fig. 5, we report the transmittance of two different designs vs. the angle of incidence θ_0 . The two devices have the same operation frequency f_0 but are realized with different ceramic materials. Therefore, they achieve a balanced condition between symmetric and anti-symmetric scatterers for different impinging angles. As expected, the all-dielectric metasurfaces behave as ultra-selective angular filters, which are able to transmit the impinging field only around the desired angle of incidence. Specifically, for the second design working around $\theta_0=30^\circ$, the obtained -3dB angular bandwidth is lower than 10° , while the attenuation for normal incidence is higher than 15 dB. This value can be further enhanced by properly optimizing the overall geometry of the structure.

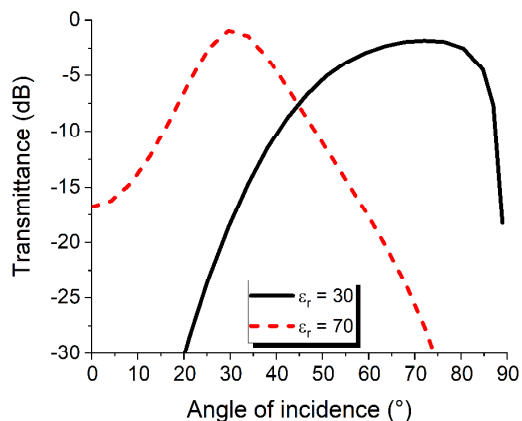


Figure 5. Transmittance (in dB) of the designed all-dielectric metasurface vs. the impinging angle for different material permittivity. The transmittance is evaluated inside at f_0 .

To conclude, in this contribution we have described how it is possible exploiting the normal polarization sustained by all-dielectric metasurfaces for oblique incidence to design ultra-selective angular filters. This possibility, which is the result of the proper engineering of tangential and normal polarizations in a Mie-based structure, confirm that the functionalities of metasurfaces can be further enhanced by considering and engineering their intrinsic spatial dispersion.

4. Acknowledgements

This work has been developed in the frame of the activities of the contract MANTLES, funded by the Italian Ministry of University and Research as a PRIN 2017 project (protocol number 2017BHFZKH).

References

[1] S.A. Tretyakov, "Metasurfaces for general transformations of electromagnetic field," *Philosophical Transactions A*, **373**, 2013, 20140362.

[2] A.I. Kuznetsov, A.E. Miroschnichenko, M.L. Brongersma, Y.S. Kivshar, and B. Luk'yanchuk, "Optically resonant dielectric nanostructures," *Science*, **354**, 2016, 2472.

[3] R. Jacobsen, A. Lavrinenko and S. Arslanagic, "Water-based metasurfaces for effective switching of microwaves," *IEEE Antennas Wireless Propagation Letters*, **17**, 2018, pp. 571-574.

[4] A. Monti, A. Alù, A. Toscano, F. Bilotti, "Design of High-Q Passband Filters Implemented through Multipolar All-Dielectric Metasurfaces," *IEEE Transaction on Antennas and Propagation*, **69**, 2021, pp. 5142-5147

[5] R.P.-Domínguez et al., "Generalized Brewster effect in dielectric metasurfaces," *Nature Communication*, **7**, 2016, 10362.

[6] A. Cordaro, H. Kwon, D. Sounas, A.F. Koenderink, A. Alù, and A. Polman, "High-index dielectric metasurfaces performing mathematical operations," *Nano Letters*, **19**, 2019, pp. 8418-8423.

[7] X. Chen et al., "Magnetic Metamirrors as Spatial Frequency Filters," *IEEE Transactions on Antennas and Propagation*, **68**, 2020, pp. 5505-5511.

[8] A. Monti, A. Alù, A. Toscano, F. Bilotti, "Surface Impedance Modeling of All-dielectric Metasurface," *IEEE Transaction on Antennas and Propagation*, **68**, 2020, pp. 1799-1811.

[9] M. Yazdi, and M. Albooyeh, "Analysis of Metasurfaces at Oblique Incidence," *IEEE Transaction on Antennas and Propagation* **65**, 2017, pp. 2397-2404.

[10] M. Albooyeh, D.-H. Kwon, F. Capolino, and S. A. Tretyakov, "Equivalent realizations of reciprocal metasurfaces: Role of tangential and normal polarization," *Physical Review B*, **95**, 2017, 115435.

[11] Skyworks Technical Ceramics. Available at: <https://www.skyworksinc.com/en/Products/Technica1-Ceramics/>.

[12] P.H. Bolivar, et al., "Measurement of the dielectric constant and loss tangent of high dielectric-constant Materials at terahertz frequencies," *IEEE Transaction on Microwave Theory and Techniques*, **51**, 2003, pp. 1062-1066.